

Amyloid Analyzer - A software assistant for qualitative and quantitative analysis of Florbetaben PET scans

F. Weiler¹, V. Dicken¹, J. Strehlow¹, B. Geisler¹, M. Scarpa², M. Pessel², A. Stephens³, and H. K. Hahn¹

¹Fraunhofer MEVIS, Bremen, Germany

²Bayer Healthcare, Berlin, Germany

³Piramal Imaging, Berlin, Germany

Abstract

Amyloid imaging is currently on the verge of becoming a vital imaging biomarker for the diagnosis and progress-monitoring of Alzheimer's disease. It is a positron emission tomography (PET) imaging technique based on tracers binding to β -amyloid plaques in the brain. These plaques are known to accumulate over time in the gray matter of the brains of AD patients. Images acquired with an amyloid binding tracer can be difficult to interpret, especially for cases showing an early stage of the disease. Also, precise quantification is challenging, because the cortical gray matter can not be well delineated from the images. In this work, we present a software assistant targeted at both qualitative and quantitative analysis of amyloid PET scans. It has been designed with the aim to be easy to use and integrate well into clinical workflows, while at the same time providing solid quantitative results for use e.g. in pharmaceutical trials.

Categories and Subject Descriptors (according to ACM CCS): I.3.8 [Computer Graphics]: Applications—; J.3 [Life And Medical Sciences]: Health—

1. Introduction

Alzheimer's disease (AD) is an epidemiologically highly relevant neurodegenerative disease. It is the most common type of dementia accounting for approximately 60% of all dementias world-wide. The generally increasing life expectancy in the western world in combination with a highly increased incidence of AD from the 65th year of life onward, it is expected that by the year 2050 approximately one in 85 people will be affected by the disease globally.

Until now, there is no cure for the disease. However, research on disease modifying therapies is being pushed heavily with a variety of pharmaceutical studies and pre-clinical trials currently being conducted. In order to assess the efficacy of potential drugs, clinical or imaging biomarkers are required. One such biomarker is provided by amyloid PET imaging. β -amyloid plaques are known to play a critical role in the process of cellular decline in the gray matter of brains affected by AD. Accumulation of these plaques progresses over time and is expected to begin already several years prior to the onset of clinical symptoms. As a result, amyloid PET imaging holds high potential in both early detection as well as monitoring of the course of the disease.

Currently, there are three Flour-18 labeled amyloid binding PET tracers in development. One of these is Florbetaben (FBB), for which the software assistant presented here has been optimized. Interpretation of images acquired with FBB requires the reader to undergo thorough training in order to learn and understand the image characteristics. The tracer has a lipophilic character, which causes it to bind unspecifically to white matter brain tissue. β -amyloid plaques however accumulate only in the cortical gray matter areas of the brain. Consequently, for pathological cases the tracer will also accumulate in the gray matter areas. The challenge with reading such images lies in answering the question how far the FBB-signal extends from the white matter into the cortex. This question is relatively simple to answer for highly pathologic case, where high signal is observed throughout the brain. But for beginning cases this requires an experienced reader to evaluate. Also, it requires some efforts to draw quantitative measures from such images without the use of specialized algorithms. These measures, however, are essential for monitoring the progression of the disease and eventual therapy response, i.e. during the course of clinical trials.

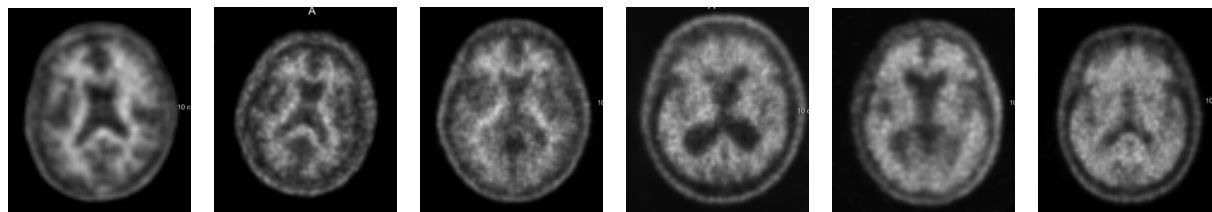


Figure 1: Several PET images acquired with Florbetaben. Extension of signal into the cortical areas rises from left to right, reflecting the state of the pathology.

To facilitate this process, a statistical analysis method is applied which is based on an approach initially developed for the analysis of FDG-PET brain scans. Here, instead of directly interpreting the PET image itself, the image is compared to a normal template. A simple statistical z-test is performed for each voxel of the image in question, which yields the amount of deviation from the normal group in terms of standard deviations. In the nuclear medicine community, this is typically referred to as a z-score. Such resulting z-score images can be either visualized using false colors for simplified qualitative interpretation, or they can be quantified over regions-of-interest within the brain.

In this work, we present a software assistant which aims to deliver

- a simple to use, workflow optimized tool for *qualitative* assessment, and
- a robust automated *quantitative* analysis for AD-relevant brain areas

A brief technical description of the methods and the resulting software is presented in the following sections.

2. Methods

For applying the method of statistical analysis presented here, a normal template is required to which individual images can be compared to. We used 50 amyloid negative FBB scans acquired as part of a clinical trial conducted by Bayer Healthcare [BGD*11] to create our template. These images were registered into the MNI coordinate system, normalized to standardized uptake value ratios (SUV-r), and averaged to obtain a mean and a standard deviation image of the normal population. SUV-r normalization is done by normalizing all voxel intensities to the average intensity of cerebral gray matter. Because all images are aligned in MNI space, an anatomical atlas can easily be applied to identify the cerebellum and other regions of the brain. For this work, we created a custom atlas based on the publicly available AAL atlas [TMLP*02]. We have coarsened and partly modified the regions labeled in AAL to better account for the image resolution of the PET scans, while keeping anatomical key regions of AD intact.

2.1. Image Processing

The image processing pipeline required for our analysis consists of three steps. First, images need to be registered into the MNI coordinate system on which the normal template has been defined. Afterwards, image intensity values need to be normalized such that the average SUV for the cerebellum becomes 1.0. Finally, the transformed and normalized image can be evaluated against the normal template to calculate a z-score map.

The challenge in image registration of amyloid PET scans lies in robustly identifying the brain from the incoming PET data. This is founded in the tracers characteristic of binding to the white matter and extending into gray matter in pathological cases only. This causes the primary difference between a positive and a negative scan to depend on the size of the white matter print in the image. A naive registration algorithm would try to compensate for this size effect, by either shrinking or expanding the image. We have implemented an image processing pipeline which robustly identifies the border between the skull and the brain in such scans, regardless of the presence of pathological tracer signal. The resulting ridge map is then used as a feature image for a linear registration, effectively resulting in a very robust, automated registration procedure. The algorithm has a running time of approximately 25-30 seconds on standard PC hardware.

After the image has been aligned into MNI space, the cerebellum can be extracted from the atlas. The histogram of the underlying image data is analyzed to extract the mean value of cerebellar gray matter, which is then used to normalize the image.

Finally, the z-score map can be calculated by evaluating for each voxel the difference between the mean of the normal template, divided by its standard deviation. The resulting values measure the deviation in terms of standard deviations of an assumed normal distribution. Typically, a value of 2.5 or above is then considered to be a significant deviation indicating a pathologically high tracer uptake.

2.2. Z-Score Quantification

Quantification of the z-score map is done based on an analysis of the tracer uptake found in individual brain re-

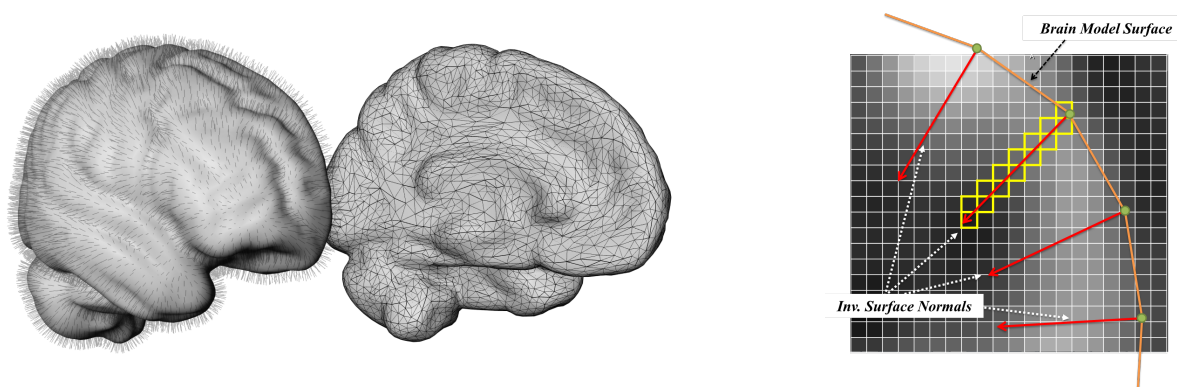


Figure 2: Schematic illustration of the surface projection algorithm.

gions. These regions have been defined by a neuroradiologist, based on the freely available AAL atlas. As the granularity of this atlas is too high to make precise statements on the spatially low resolution of the PET scans, the regions provided by AAL have been collapsed into 16 regions per hemisphere. These new regions have been defined with the known course of progression of the disease in mind, in order to keep important areas intact.

Quantification of z-scores over these areas is done by analysis of the underlying histogram of each region. We evaluate different parameters, such as the 90% quantile, or the percentage of voxels above the significance threshold. By adjusting these values for the expected ratios of gray matter to white matter, a regional z-score can be calculated. This indicates the amount of amyloid-bound tracer uptake for each region.

2.3. Surface Projection

For a more intuitive, qualitative assessment of an image, we have implemented an algorithm which projects z-scores from the cortical surface onto a 3D brain model. The approach is an adaption of the method proposed by [MFK*95]. The brain model has been extracted from the ICBM 152 brain template provided by MNI [ECM*93]. A separate model has been created for each hemisphere. This allows to also look at the cortical areas located at the inner side of each hemisphere. Especially the medial parietal lobe located there is known to be affected already during an early stage of the disease.

The projection is calculated by sampling the z-score map along the inverted surface normals of the 3D model. Sampling is done using a cubic interpolation scheme along the paths. For each normal, a ray is cast 15mm into the depth of the brain. Along this path, a maximum intensity projection is calculated and the resulting value is mapped as a color value at the corresponding vertex. The algorithm is implemented

on the CPU and runs less than one second for approximately 20.000 vertices of the brain model. In our application this is not a time critical step.

Figure 2 illustrates the algorithm. On the left, the brain model is shown with the surface normals and the triangular mesh indicated, each for one hemisphere. The image on the right side shows schematically in 2D how the resampling along the inverted surface normals is performed.

The resulting 3D visualization mode is primarily meant as way to gain a quick qualitative assessment of a case. The brain can be rendered either in its original anatomy, revealing a view at the cortical surface, or in an exploded view offering a look at the inner structures. For reporting purposes, screenshots can be generated showing the whole brain from different perspectives, thus allowing to see the complete cortical surface in one view. The ease to grasp visualization of results can potentially also be useful when discussing results of an examination with the patient or his relatives.

3. Workflow and User Interface

The application has been designed with the aim of providing an easy to use tool that should integrate well into established clinical workflows. As such, a high degree of automation as well as short overall processing times were given requirements. We have implemented a linear workflow consisting of four steps, along which the user can step through a case.

The first step is the case- and study-manager. From here, the user can open cases and define the actual image that should be analyzed. If available, additional MRI or CT images can be defined for a case, although they are not required to perform the analysis.

The second step serves as a quality check for the result of the automatic registration. Two visualization modes are offered to simplify judgment on the quality of the results. An interactive widget is offered to correct the registration, for

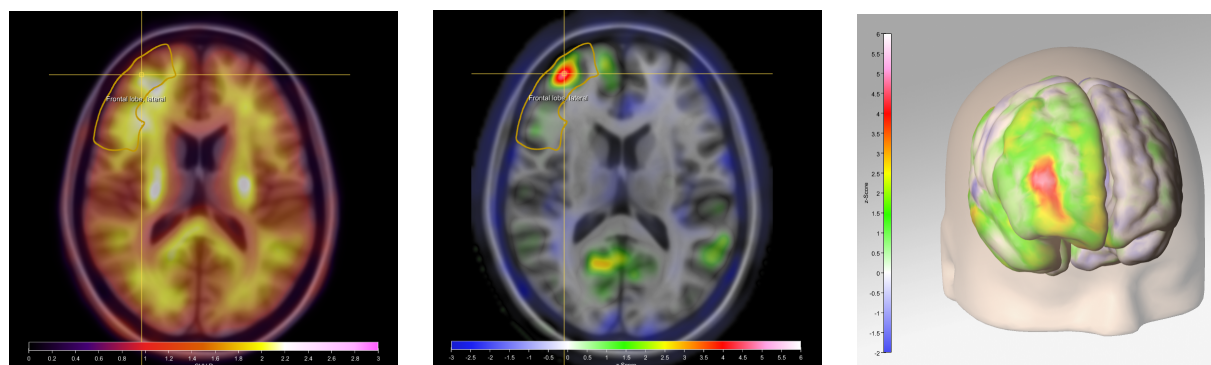


Figure 3: Results for one case showing an early stage of progression. While the SUV-r image to the left appears almost normal, the z-score map clearly identifies a region with abnormally high tracer uptake. This area can be immediately identified in the 3D surface projection shown to the right.

cases, where a suboptimal registration result was achieved automatically. During our evaluation, this affected less than 5% of all cases (150 cases in total).

The third step serves for the actual analysis. It provides synchronized 2D viewers showing both the SUV-r image and the z-score map as color overlays over either the patients MRI, or a template MRI. Additionally, the 3D viewer can be activated showing the surface projection rendering. For interaction, the user has the option to toggle different atlas visualization modes and switch between voxelwise or regional quantification. A tool for manually delineating ROIs will be added in a future version, following requests from a small user evaluation.

Finally, the fourth step is used for reporting the results of the analysis. A table with all quantitative measures is automatically generated and added into a reporting template along with a set of automatically generated screenshots. Here, the user has the option to type in his diagnosis and findings. The reporting system has been implemented using HTML templates, which can easily be adapted to the custom style e.g. that of a certain clinical site.

4. Results

The software was used to evaluate 150 cases from Bayer's phase-II study for Florbetaben. The results of a z-score reading by four non-expert readers, as well as one neuroradiologist were compared with published results. Compared to the clinical diagnosis (obtained from neurological exams), the amateurs achieved sensitivity and specificity values comparable to those of the experts, partly even surpassing them. Further evaluations are currently being performed. Also, a usability workshop has been scheduled, where experts from the field of nuclear medicine are invited to provide feedback on the overall usability of the software and the quality of the analysis.

There are a number of missing features that have already been requested by users. These mostly address options for a more flexible definition of finding results, by means of adding custom screenshots or manual delineations of ROIs. Also, there is still room for improvement with the registration, especially for highly atrophic cases often seen during later stages of the disease. However, the overall feedback received so far has been overwhelmingly positive. Especially, the combination of ease of use with detailed, quantitative results has been highlighted by all users so far.

References

- [BGD*11] BARTHEL H., GERTZ H.-J., DRESEL S., PETERS O., BARTENSTEIN P., BUERGER K., HIEMEYER F., WITTEMER-RUMP S. M., SEIBYL J., REININGER C., SABRI O.: Cerebral amyloid- β pet with florbetaben (18f) in patients with alzheimer's disease and healthy controls: a multicentre phase 2 diagnostic study. *The Lancet Neurology* 10, 5 (2011), 424 – 435. URL: <http://www.sciencedirect.com/science/article/pii/S1474442211700771>, doi:10.1016/S1474-4422(11)70077-1. 2
- [ECM*93] EVANS A. C., COLLINS D. L., MILLST S. R., BROWN E. D., KELLY R. L., PETERS T. M.: 3D statistical neuroanatomical models from 305 MRI volumes. Symposium I.-N. S., Conference M. I., (Eds.), pp. 1813–1817. 3
- [MFK*95] MINOSHIMA S., FREY K. A., KOEPPPE R. A., FOSTER N. L., KUHL D. E.: A diagnostic approach in alzheimer's disease using three-dimensional stereotactic surface projections of fluorine-18-fdg pet. *Journal of Nuclear Medicine* 36, 7 (1995), 1238–1248. URL: <http://jnm.snmjournals.org/content/36/7/1238.short>, arXiv:<http://jnm.snmjournals.org/content/36/7/1238.full.pdf+html>. 3
- [TMLP*02] TZOURIO-MAZOYER N., LANDEAU B., PAPANATHANASSIOU D., CRIVELLO F., ETARD O., DELCROIX N., MAZOYER B., JOLIOT M.: Automated anatomical labeling of activations in spm using a macroscopic anatomical parcellation of the mni mri single-subject brain. *NeuroImage* 15, 1 (2002), 273 – 289. URL: <http://www.sciencedirect.com/science/article/pii/S1053811901909784>, doi:10.1006/nimg.2001.0978. 2